

# Chapter 5

## Longer MEMS Switch Lifetime Using Novel Dual-Pulse Voltage Driver

Lai Chean Hung and Wallace S.H. Wong

**Abstract** A novel dual-pulse voltage driver has been proposed to reduce dielectric charging in micro-electromechanical system (MEMS) switch, leading to a longer switch lifetime. Mathematical and transient circuit models have been utilized to simulate dielectric charging in the RF MEMS switch, enabling the analysis of charge built-up at the switch dielectric and substrate brought about by the actuation voltage curve used. The proposed dual-pulse actuation signal has shown to improve the lifetime of the RF MEMS switch as it minimizes the charge built-up during its long continuous operation. Practical experiment on the commercial TeraVicta TT712-68CSP MEMS switch shows that the proposed actuation voltage can reduce the pull in/out voltage shift and therefore prolong the switch lifetime. The technique has also shown to reduce switching bounces.

**Keywords** Radio frequency (RF) · micro-electromechanical system (MEMS) · dielectric · charging · reliability · lifetime

### 5.1 Introduction

Microelectromechanical Systems or MEMS switch is becoming the preferred choice for RF switching due to its outstanding performance when compare to the conventional solid state RF switch such as p-i-n diodes or FET transistor. RF MEMS switch has very low insertion loss but high isolation and consumes minimal power in the microwatts rather than the milliwatts that solid state switches require. However, unlike its solid state counterparts, due to the electro-mechanical nature the MEMS switch suffers from shorter lifecycle ranging from 100 million to 10 billion cycles only [1].

---

L.C. Hung (✉) and W.S.H. Wong  
School of Engineering & Science, Swinburne University of Technology (Sarawak campus),  
Jalan Simpang Tiga, 93350 Kuching, Sarawak, Malaysia  
e-mail: [clai@swinburne.edu.my](mailto:clai@swinburne.edu.my); [wwong@swinburne.edu.my](mailto:wwong@swinburne.edu.my)

In capacitive membrane switches, the main life-limiting mechanism is dielectric charging trapped within the switch dielectric layer due to the high actuation voltage required to actuate the switch [2, 3]. When sufficient actuation voltage is applied to the electrodes beneath the membrane, the membrane is pulled down towards the dielectric layer by electrostatic force, creating a capacitive short. Over time and repeated ON-OFF cycles charges are trapped in the dielectric layer and the substrate of the switch, pulling the membrane to the dielectric even without any actuation voltage applied.

This chapter presents an analysis on the charge trapped in the switch using mathematical and transient circuit models of the charge built-up [5]. Then the implementation of a novel dual-pulse actuation voltage which reduces charge built-up and therefore extends the lifetime of the switch will be presented. The analysis is then corroborated through experiment where the commercially available TeraVista (now defunct) TT712-68CSP MEMS switch is shown to experience less pull in/out voltage shift during long term operation, even when the switch is of metal-to-metal (ohmic) type.

## 5.2 Dielectric Charging

A typical capacitive membrane switches generally require 30–50 V of actuation voltage which will form a very high electric field in a region of 100 MV/m across the dielectric layer. In this condition, it is possible for charges to tunnel across the dielectric and become trapped within the dielectric layer through a process similar to that of Frenkel-Poole emissions in thin insulating films [2], where the charged trapped is exponentially related to the applied electric field. During switching ON, charges will be accumulated on the surface of the dielectric or even on the bulk of the substrate since the recombination time for these charges can be very long and there is a lack of conduction path to drain off the trapped charges. When the trapped charges build up to a level that is just enough to hold the membrane to the dielectric layer even without the presence of actuation voltage, the switch is stuck at the ON state.

The built-up charge also affects the pull-in voltage  $V_{pi}$  and pull-out voltage  $V_{po}$  of the switch. Pull-in voltage  $V_{pi}$  is the threshold voltage that the actuation voltage must exceeds so that the electrostatic force generated will be greater than the restoring force of the switch membrane and closes the switch. Once the switch closes, the electric field will be higher due to the smaller gap between the membrane and electrodes. Hence, the switch will only open when the applied voltage is reduced to below the pull-out voltage,  $V_{po}$ .

The trapped charges change the magnitude of the electric field presents in the dielectric layer and thus the generated electrostatic force as well. In case of a positive actuation voltage, positive charges will tunnel into the dielectric layer due to the high electric field across the gap. The trapped charges will generate electrostatic force itself and increase the net amount of electrostatic force between the membrane

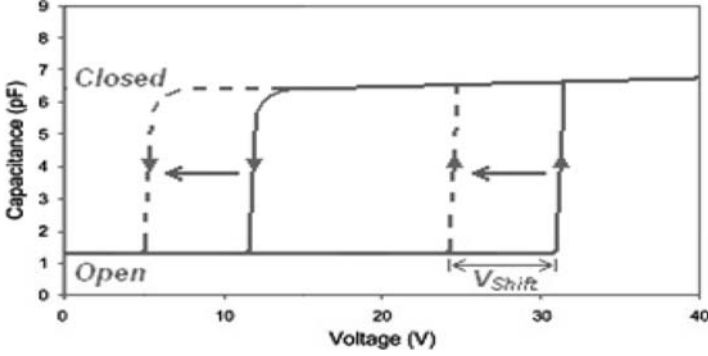


**Fig. 5.1** C-V curve of capacitive RF MEMS switch before (*solid line*) and after continuous actuation (*dotted line*) [4]

and electrodes. This reduces the amount of external force/voltage needed to pull down the switch membrane. The net effect of injected positive charges is therefore a negative shift of the switch C-V curve as shown in Fig. 5.1, which in turn affects the pull-in and pull-out voltages where  $V_{pi} = V_{pi} - V_{shift}$  and  $V_{po} = V_{po} - V_{shift}$ . Since  $V_{shift}$  is proportional to the amount of trapped charge, the longer the switch has been in operation, the more charges are accumulated and  $V_{shift}$  increases. The switch will fail when  $V_{po}$  in positive region becomes negative. In that case, the switch will be in the closed state even at 0 V.

## 5.3 Modeling of Dielectric Charging

### 5.3.1 Mathematical Model

Dielectric charging for each ON time of the operating cycle can be modeled as [3]:

$$Q_C = \sum_{J=1,2} Q_J \times (1 - \exp(-(t_{on} + t_{eJ})/\tau_{CJ})) \quad (5.1)$$

where  $Q_J$  is the steady state charge density for Jth trap species (there are two types only,  $J = 1$  and  $J = 2$ ),  $t_{on}$  is the ON time duration for one cycle,  $\tau_{CJ}$  is the charging time constant for Jth trap species and  $t_{eJ}$  is the equivalent time required to charge the dielectric to the value just before the present ON time. The steady state charge density  $Q_J$  for the Jth trapped species when absolute voltage  $V$  is applied is given by:

$$Q_J = Q_{0J} \times \exp(V/V_{0J}) \quad (5.2)$$

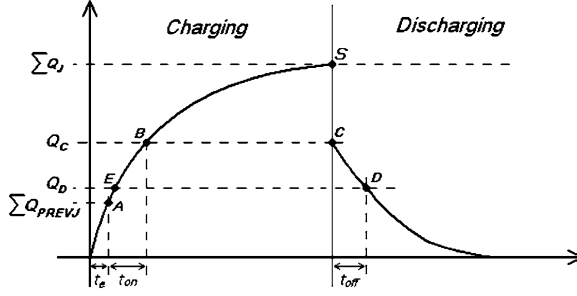


**Fig. 5.2** Dielectric charging and discharging under square wave actuation voltage after one operating cycle, the charge density increases from the initial-state A to the end-state E

where  $Q_{0J}$  and  $V_{0J}$  are fitting parameters. Dielectric discharging can be model as:

$$Q_D = \sum_{J=1,2} Q_{PREVJ} \times \exp(-t_{off}/\tau_{DJ}) \quad (5.3)$$

where  $Q_D$  is the charge accumulated after the OFF time duration,  $Q_{PREVJ}$  is the amount of charges trapped in the dielectric just before the OFF time for Jth trap species,  $t_{off}$  is the OFF duration and  $\tau_{DJ}$  is the discharging time constant for Jth trap species. By iterating Eqs. (5.1) and (5.3), the accumulation of charge over many operating cycles can be obtained. Figure 5.2 depicts the dielectric charging and discharging curve under a square wave ON-OFF actuating voltage [3]. The trapped charge at the beginning of each operating cycle can be somewhere between empty and full, represented by point A on the charging curve. When the switch is turned ON, the amount of charges increases to point B ( $Q_C$ ) at the end of the ON time, which can be calculated by using Eq. (5.1). Once the switch is turned OFF, the charges trapped inside the dielectric start to discharge from point C on the discharging curve. At the end of the OFF time, the dielectric is discharged to point D ( $Q_D$ ) which can be calculated by Eq. (5.3). For the next cycle, point D is mapped back onto point E on the charging curve. Thus, the net amount of charges accumulated on the dielectric after one operating cycle is equals to point E minus point A.

Figure 5.3 shows the accumulated charge simulated using the above model over a long operating cycle. The switch model used is similar to that in [3], using similar extracted parameters as shown in Table 5.1. The switch is operated using square wave of 100 Hz, 50% duty cycle. The voltage shift due to dielectric charging can then be calculated by using Eq. (5.4):

$$\Delta V = \frac{dQq}{\epsilon_0 \epsilon_r} \quad (5.4)$$

where,  $\Delta V$  is the voltage shift  $V_{shift}$  due to dielectric charging,  $d$  is the distance between the centroid of the charge sheet (dielectric) and the top electrode (switch membrane),  $Q$  is the charge density modeled by Eqs. (5.1) and (5.3),  $q$  is the

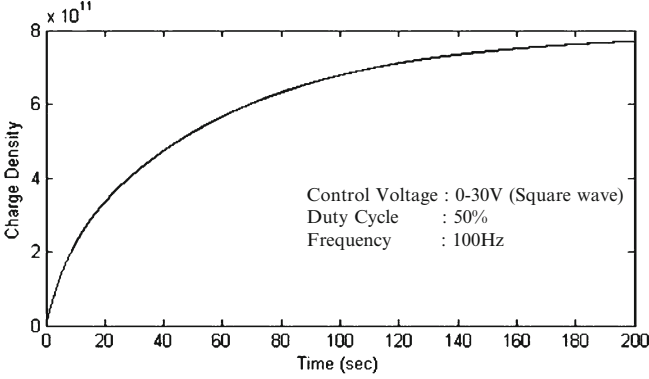


**Fig. 5.3** Dielectric charge density accumulated over 200 s stressed by 0–30 V square wave actuation signal

**Table 5.1** Extracted model parameters

$J$	$\tau_C$ (s)	$\tau_D$ (s)	$Q_0$ (q/cm <sup>2</sup> )	$V_0$ (V)
1	6.6	6.8	$3.1 \times 10^{10}$	13
2	54	62	$1.6 \times 10^{11}$	15

electron charge,  $\varepsilon_O \varepsilon_r$  is the permittivity of dielectric. This equation calculates how much the  $V_{pi}$  and  $V_{po}$  have been shifted based on the density trapped charge and therefore the switch failure due to dielectric charging can be modeled.

### 5.3.2 Equivalent Circuit Model

In order to analyze the dielectric charging under a more complex actuation voltage waveform, a SPICE model was implemented by Yuan et al. by using two RC sub-circuits to simulate the charging and discharging behavior of the dielectric [5]. As shown in Fig. 5.4, the two sets of RC circuit represent the two trapped species with different charging and discharging time constants. Dielectric charging is represented by the charging of both capacitors,  $C_1$  and  $C_2$ . Both capacitors were set to unity so that the resistances directly correspond to the charging and discharging time constants.  $R_{C1}$  and  $R_{D1}$  represent the charging and discharging time constants for  $J = 1$ , and  $R_{C2}$  and  $R_{D2}$  represent the charging and discharging time constants for  $J = 2$ . Diodes in the circuit were used to direct charge flow. The total charge trapped in the dielectric can be obtained by adding the charge accumulated on the unity capacitors ( $C_1$  and  $C_2$ ). Two voltage sources,  $V_1$  and  $V_2$  were implemented to represent the steady state charge density for different trap species. The value of the voltage sources are determined by Eq. (5.2).

The simulated result by using the equivalent circuit model is shown in Fig. 5.5. In this figure, it is shown that the result from the equivalent circuit model is very

**Fig. 5.4** Equivalent-circuit model for transient circuit simulation. Voltage dependence of the steady-state charge densities was implemented in the two voltage sources  $V_1$  and  $V_2$

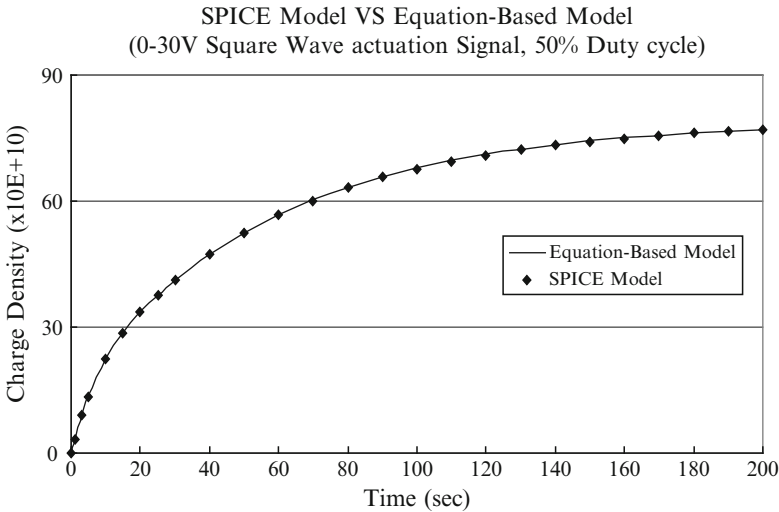
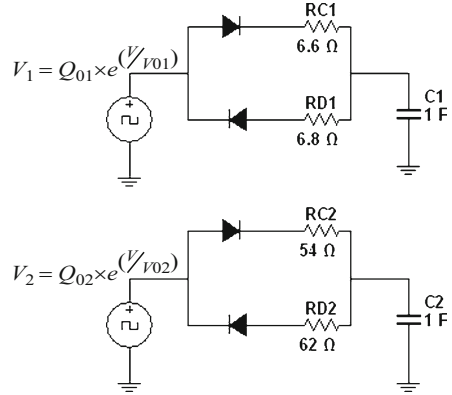


**Fig. 5.5** Dielectric charging curve over 200 s at 100 Hz switching modeled by using equation-based model compared to the spice model

close to the one predicted by the equation-based model. Hence, dielectric charging effect for complex waveform such as dual-pulse actuation signal can be obtained using the Transient SPICE model by simply changing the shape of the two voltage sources  $V_1$  and  $V_2$ .

### 5.4 Dual-Pulse Actuation Signal

Goldsmith et al. has proposed a dual-pulse actuation voltage to reduce dielectric charging [2]. The waveform comprises of a short high voltage pulse to pull down the switch membrane and a low-voltage pulse to hold the membrane at ON state.

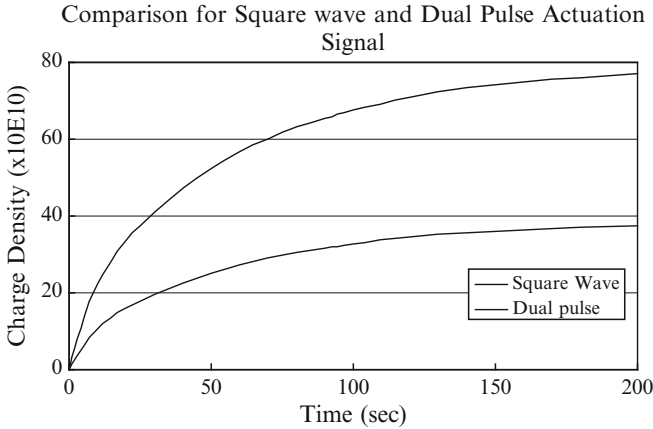


**Fig. 5.6** Comparison of dielectric charging effect between a 100 Hz, 0–30 V square wave actuation signal and a 100 Hz dual pulse actuation signal

The initial high voltage must exceed the switch's pull-in voltage  $V_{pi}$ . Once the membrane has been pulled down, the increase in electrostatic force due to the smaller distance between the membrane and electrodes and the stiction force on the membrane surface reduce the required voltage to hold the switch at the ON state.

Dual-pulse actuation signal minimizes the time that high voltage is applied across the dielectric and hence reduces the dielectric charging. The effect of using dual-pulse actuation on dielectric charging is simulated using the aforementioned equivalent circuit model with some modification on the voltage sources in order to obtain the dual pulse signal. The voltage source  $V_1$  is replaced by the summation of two voltage sources with different duty cycle.  $V_{P1}$  and  $V_{P2}$  represent the peak voltages for  $J = 1$  and  $J = 2$ , and  $V_{h1}$  and  $V_{h2}$  represent the holding voltages for  $J = 1$  and  $J = 2$  respectively. Figure 5.6 shows the comparison of dielectric charging effect between a 100 Hz, 0–30 V square wave actuation signal and a 100 Hz dual-pulse actuation signal. From this figure, it is shown that the dual-pulse successfully reduces the charge trapped, leading to less  $V_{shift}$  and ultimately longer switch lifetime.

## 5.5 Novel Dual-Pulse Actuation Signal

In order to further improve the lifetime of the switch, a novel dual-pulse waveform as shown in Fig. 5.7 has been proposed. The novel actuation waveform gradually increases the actuation voltage at the beginning of the ON period, rather than a short constant pulse. This reduces the dielectric charging by effectively minimizing the time where high voltage is applied across the gap of two electrodes.

**Fig. 5.7** A typical dual-pulse actuation signal (*solid line*) and the novel dual pulsed actuation signal (*dotted line*)

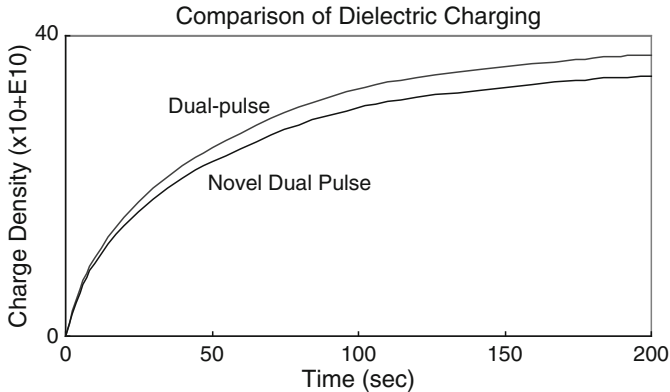
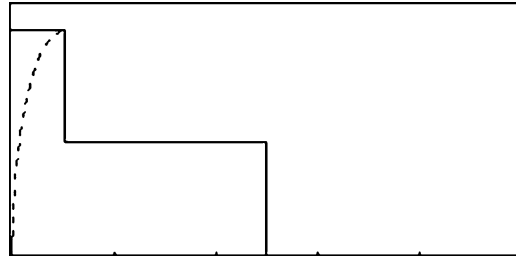


**Fig. 5.8** Comparison of dielectric charging effect between a 100 Hz, typical dual pulse actuation signal and the modified dual pulse actuation signal

One main advantage of this technique is the simplicity in its implementation. The proposed actuation voltage curve can be simply driven by adding a simple RC low pass filter after the peak voltage source. This is a straightforward analog circuit implementation suitable for any MEMS switch rather than using active component such as microcontroller and sensing circuit. Admittedly, the RC value has to be properly tuned for a particular MEMS switch so that the switch operates correctly and does not compromise too much on the delay in the switching time. This novel actuation voltage has been shown to reduce the dielectric charging even further, as shown in Fig. 5.8.

## 5.6 Experimental Setup

To test the dielectric charging effect of the RF MEMS switch, the switch is stressed under a continuous ON-OFF actuation signal. The pull-in and pull-out voltages are then measured periodically. The MEMS switch used is the commercially produced



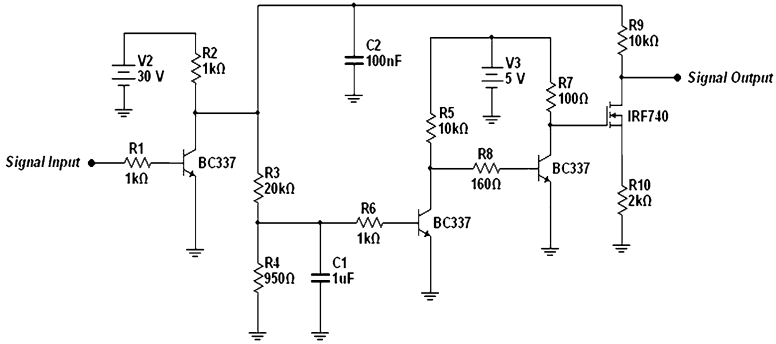


Fig. 5.9 Driver circuit for generating the novel dual-pulse actuation signal

TT712-68CSP SPDT RF MEMS switch fabricated by TeraVista. The switch was actuated at 200 Hz, with 200 ms of high voltage at 68 V followed by a 55 V holding voltage for the rest of the ON time. A sine wave (1 V peak to peak, 100 kHz) was applied at the input pin of the MEMS switch to emulate RF signal, and the output of the switch is measured using oscilloscope. The MEMS switch is hot switched.

Two RF MEMS switches were tested in the experiment, labeled SW1 and SW4. Firstly, SW1 was tested with the normal dual-pulse actuation (DP) signal while SW4 was tested with the novel dual-pulse actuation (NDP) signal for 10 min. The pull-out voltage readings were taken in every 2 min. The switches were rested for days to allow the charges trapped in the dielectric to discharge before the next test, whereby SW1 was tested with the novel dual-pulse actuation signal and SW4 was tested with the normal dual-pulse actuation signal for 10 min. A 200 Hz, 0–2 V square wave signal was applied to the driver circuit shown in Fig. 5.9 to generate the desired actuation signal. The DP and NDP actuation voltage implementation differs only in the addition of capacitor C2 in the circuit.

The actuation voltage shift for both devices under test is shown in Fig. 5.10. The graph shows that both the variation and the rate of voltage shift are higher for the normal dual-pulse actuation signal (DP) compared to the proposed novel dual-pulse actuation signal (NDP). Therefore, the experimental results support the analysis done using simulation, whereby the dielectric charging effect can be reduced by applying a gradually build-up actuation voltage.

In addition, the proposed novel dual-pulse actuation signal is observed to generate less bouncing the moment the switch closes compared to the two-step dual-pulse actuation signal. Figure 5.11 depicts the switch contact bouncing for the two different actuation schemes observed during the experiment. Though reaching the contact faster, the conventional dual-pulse actuated switch suffers from bouncing which delay the switching time significantly. Mechanical impact and contact bouncing also lead the switch mechanical failures [7, 8] in the long run.

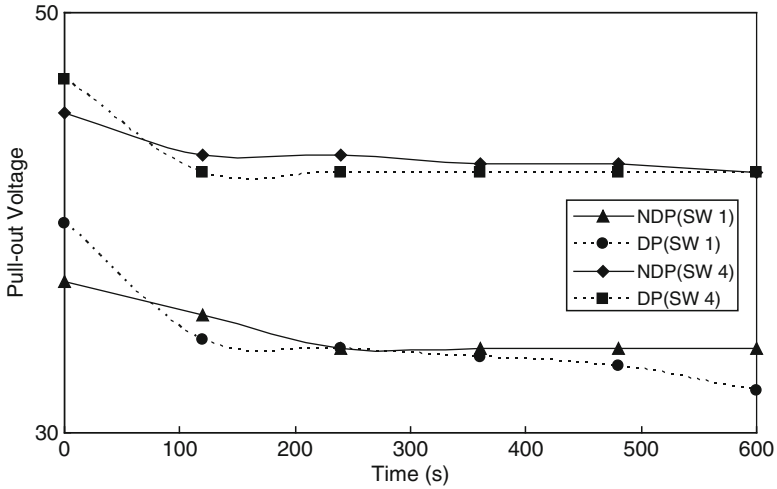


Fig. 5.10 Pull-out voltage shift for SW 1 and SW 4 over 10 min

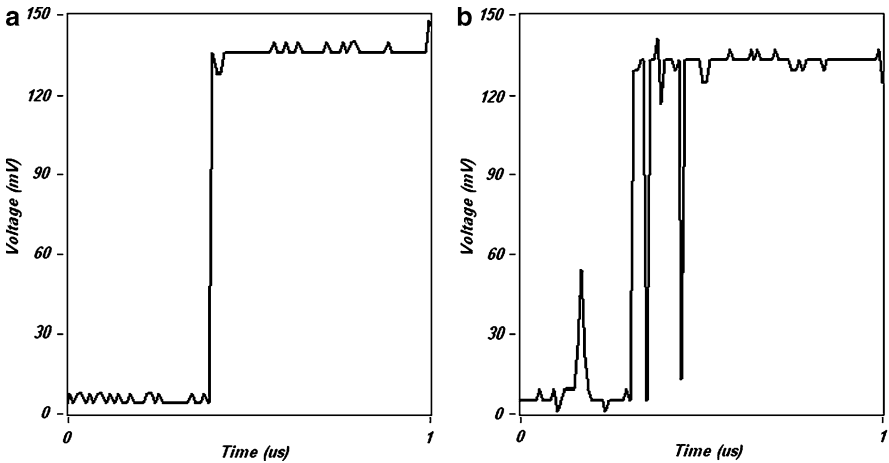


Fig. 5.11 Contact bouncing for (a) novel dual-pulse actuation signal and (b) normal dual-pulse actuation signal. A DC signal of 130 mV is applied to the switch input

## 5.7 Conclusion

Mathematical and transient circuit models of dielectric charging in a MEMS switch have been used to analyze the dielectric charging generated by different actuation voltage curves applied to the switch. From the analysis, a novel, simple to implement dual-pulse actuation voltage has been proposed to reduce the dielectric charging. Simulation using the model and experiment carried out using commercial MEMS switch have shown that the dielectric charging can be reduced, leading to less voltage shift and eventually increasing the lifetime of the MEMS switch.

## References

1. Chan, R., Lesnick, R., Becher, D., Feng, M.: Low-actuation voltage RF mems shunt switch with cold switching lifetime of seven billion cycles. *J. Microelectromech. Syst.* **12**(5), (2003)
2. Goldsmith, C.L., Ehmke, J., Malczewski, A., Pillans, B., Eshelman S., Yao, Z., Brank, J., Eberly, M.: Lifetime characterization of capacitive RF MEMS switches. *IEEE MTT-S Int. Microw. Symp. Dig.* **1**, 227–230 (2001)
3. Yuan, X., Hwang, J.C.M., Forehand, D., Goldsmith, C.L.: Modeling and characterization of dielectric-charging effects in RF MEMS capacitive switches *IEEE MTT-S Int. Microw. Symp. Dig.* (June 2005), 753–756 (2005)
4. Herfst, R.W., Steeneken, P.G., Huizing, H.G.A., Schmitz, J.: Center-shift method for the characterization of dielectric charging in rf mems capacitive switches *IEEE Trans Semiconduct Manufact* **21**(2) (May 2008)
5. Yuan, X., Peng, Z., Hwang, J.C.M. Forehand, D., Goldsmith, C.L.: A transient SPICE model for dielectric-charging effects in RF MEMS capacitive switches *IEEE Trans. Electr Device* **53**(10), 2640–2648 (October 2006)
6. Merlijn van Spengen, W., Puers, R. Mertens, R., Wolf, I.D.: A comprehensive model to predict the charging and reliability of capacitive RF MEMS switches *J. Micromech. Microeng.* **14**(4):514–521 (January 2004)
7. Patton, S.T. Zabinski J.S.: Fundamental studies of Au contacts in MEMS RF switches *Tribol Lett* **18**(2) (February 2005)
8. Czaplewski, D.A., Dyck, C.W., Sumali, H., Massad, J.E., Koppers, J.D., Reines, I., Cowan, W.D., Tigges, C.P.: A soft-landing waveform for actuation of a single-pole single-throw ohmic RF mems switch. *J. Microelectromech. Syst.* **15**(6) (December 2006)